The Power of Monitoring Stations and a CO_2 Fertilization Effect: Evidence from Causal Relationships between NDVI and Carbon Dioxide

R. K. Kaufmann*

Center for Energy and Environmental Studies and Department of Geography and Environment, Boston University, Boston, Massachusetts

L. F. Paletta

Center for Energy and Environmental Studies, Boston University, Boston, Massachusetts

H. Q. Tian

School of Forestry and Wildlife Sciences, Auburn University, Auburn, Alabama

R. B. Myneni

Department of Geography and Environment, Boston University, Boston, Massachusetts

R. D. D'Arrigo

Tree-Ring Laboratory, Lamont-Doherty Earth Observatory, Columbia University, Palisades, New York

Received 13 August 2007; accepted 6 December 2007

* Corresponding author address: R. K. Kaufmann, Center for Energy and Environmental Studies, Boston University, Boston, MA 02215.
E-mail address: kaufmann@bu.edu

DOI: 10.1175/2007EI240.1

ABSTRACT: Two hypotheses are tested: 1) monitoring stations (e.g., Mauna Loa) are not able to measure changes in atmospheric concentrations of CO_2 that are generated by changes in terrestrial vegetation at distant locations; 2) changes in the atmospheric concentration of carbon dioxide do not affect terrestrial vegetation at large scales under conditions that now exist in situ, by estimating statistical models of the relationship between satellite measurements of the normalized difference vegetation index (NDVI) and the atmospheric concentration of carbon dioxide measured at Mauna Loa and Point Barrow. To go beyond simple correlations, the notion of Granger causality is used. Results indicate that the authors are able to identify locations where and months when disturbances to the terrestrial biota "Granger cause" atmospheric CO_2. The authors are also able to identify locations where and months when disturbances to the atmospheric concentration of carbon dioxide generate changes in NDVI. Together, these results provide large-scale support for a CO_2 fertilization effect and an independent empirical basis on which observations at monitoring stations can be used to test hypotheses and validate models regarding effect of the terrestrial biota on atmospheric concentrations of carbon dioxide.

KEYWORDS: Carbon dioxide; Mauna Loa; NDVI

1. Introduction

Each year, atmospheric concentrations of carbon dioxide rise and fall through an intra-annual cycle that is associated with the balance between photosynthesis and respiration in the terrestrial biota (Francey et al. 1995; Keeling et al. 1996; Morimoto et al. 2000). The terrestrial biota can change the amplitude and timing of the intra-annual cycle via several mechanisms including 1) a fertilization effect due to the increased concentration of atmospheric carbon dioxide (Kohlmaier et al. 1989), 2) seasonal shifts in the phasing of photosynthesis and respiration (Chapin et al. 1996), and/or 3) changes in the length or intensity of the growing season at high latitudes (Myneni et al. 1997a).

While the role of the terrestrial biota in the intra-annual cycle is not in dispute, the ability to link biotic activity and atmospheric measurements of carbon dioxide at distant monitoring stations is a point of contention. Simulations generated by models of atmospheric transport indicate that interannual changes in atmospheric circulation disrupt the link between biotic changes and measurements taken at distant stations (Murayama et al. 2004). Based on these results, Murayama et al. (Murayama et al. 2004) argue that Northern Hemisphere observational sites are not sensitive to changes in terrestrial carbon fluxes, except as they occur close to the site. If correct, this disconnect would undermine efforts to validate models of the terrestrial biosphere by comparing their results with observations at Mauna Loa (e.g., Randerson et al. 1997) and statistical analyses that relate changes in terrestrial biota to changes in atmospheric concentrations at distant monitoring stations (e.g., Buermann et al. 2007).

Here, we establish the foundation for empirical analyses of the relationship between terrestrial vegetation and atmospheric CO_2 at distant monitoring stations by testing two hypotheses:

1) Monitoring stations (e.g., Mauna Loa) are not able to measure changes in atmospheric concentrations of CO_2 that are generated by changes in terrestrial vegetation at distant locations.

2) Changes in the atmospheric concentration of carbon dioxide do not affect terrestrial vegetation at large scales under conditions that now exist in situ.

We say foundation because rejecting hypothesis number 1 (as proposed by Murayama et al. 2004) would provide an empirical basis on which observations at monitoring stations could be used to test hypotheses and validate models regarding the effect of the terrestrial biota on atmospheric concentrations of carbon dioxide. Rejecting hypothesis number 2 would provide large-scale empirical support for efforts to quantify a CO_2 fertilization effect at smaller scales. Finally, rejecting both hypotheses would allow more sophisticated analyses in which scientists identify factors that cause changes in vegetation that affect atmospheric carbon dioxide and vice versa.

Hypothesis number 1 and hypothesis number 2 are tested by estimating statistical models of the relationship between satellite measurements of the normalized difference vegetation index (NDVI), which proxies terrestrial vegetation, and the atmospheric concentration of carbon dioxide measured at Mauna Loa, Hawaii, and Point Barrow, Alaska. To go beyond simple correlations, we use the notion of Granger causality. Results indicate that we are able to identify locations where and months when disturbances to the terrestrial biota "Granger cause" atmospheric CO_2. We are also able to identify locations where and months when disturbances to the atmospheric concentration of carbon dioxide generate changes in NDVI. Together, these results reject hypothesis number 1 and hypothesis number 2.

These results and the methods used to obtain them are described in five sections. Section 2 describes how the notion of Granger causality can be used to study the relationship between atmospheric CO_2 and terrestrial biota in a way that goes beyond simple statistical correlations. Sections 3 and 4 describes results that allow us to map the spatial and temporal effect of changes in the terrestrial biota on atmospheric concentrations of CO_2 and vice versa. Section 5 concludes with a description of future research that may allow us to identify the factors that disturb terrestrial vegetation in a way that changes the global carbon cycle and how these disturbances feed back on the terrestrial biota.

2. Methodology

We analyze the relationship among station measurements of atmospheric carbon dioxide, satellite measurements of NDVI, anthropogenic carbon emissions, and aerosol optical depth (AOD) using the notion of Granger causality. Clive Granger was awarded the 2003 Nobel Prize in Economics in part for his statistical notion of causality; nevertheless, we recognize that Granger causality is not equivalent to the meaning of causality in physical sciences. Despite this difference, Granger causality goes well beyond the simple notion correlation (Granger 1969). As such, Granger causality has been used to analyze interconnected systems that cannot be manipulated using the traditional experimental approach, such as the linked climate/biotic system (e.g., Wang et al. 2006; Kaufmann et al. 2003).

The statistical methodology proceeds in three steps. In the first step, we estimate a vector autoregression (VAR) in which NDVI and the atmospheric concentration of carbon dioxide are endogenous variables. In the second step, we test for Granger causality by calculating a test statistic to evaluate a restriction that eliminates

lagged values of the potentially causal variable. Values of the test statistic that reject this restriction identify months when and locations where there is a causal relationship between atmospheric CO_2 and NDVI. A third step repeats this procedure with NDVI data at different spatial resolutions to ensure that the results are robust.

2.1. Data

We compile monthly data for NDVI, atmospheric carbon dioxide, aerosol optical depth, and annual data for anthropogenic carbon emissions. NDVI is used as a proxy for terrestrial vegetation because it closely correlated with the fraction of photosynthetically active radiation absorbed by plant canopies (Myneni et al. 1995), leaf area index (Myneni et al. 1997b), potential photosynthesis (Nemani et al. 2003), biomass (Myneni et al. 2001), and the physiological status of trees (Kaufmann et al. 2004). We use the 15-day NDVI dataset at 8-km resolution (January 1982 to December 2003) for vegetated pixels north of 30°N that is produced by the Global Inventory Modeling and Mapping Studies group (GIMMS) from measurements of the Advanced Very High Resolution Radiometer (AVHRR) on board the *NOAA-7*, *NOAA-9*, *NOAA-11*, and *NOAA-14* satellites (Zhou et al. 2001). Nonvegetation effects are reduced by analyzing only the maximum NDVI value within each 15-day interval, which is termed compositing (Holben 1986). The quality of the GIMMS NDVI dataset between 40° and 70°N is assessed by Zhou et al. (Zhou et al. 2001), who conclude that the data are of satisfactory quality. The 15-day composites are averaged to generate monthly values. Individual pixels are aggregated to grid cells of four sizes: 1° × 1° (4 pixels × 4 pixels), 2° × 2°, 3° × 3°, and 5° × 5°.

Reflectances in both the visible and near-infrared channels are affected by aerosols. Both tropospheric and stratospheric aerosols increase atmospheric optical depth and therefore reduce NDVI. The magnitude of this effect cannot be derived from quantitative characteristics of tropospheric aerosols because they are spatially and temporally variable (Gutman 1999). Stratospheric aerosols associated with volcanic eruptions, however, tend to have latitudinally homogeneous distributions within two months of injection and decrease slowly with time. The availability of stratospheric aerosol data makes it possible to correct the GIMMS NDVI data for the effect of aerosols associated with volcanic eruptions. To assess their effect, we use data on stratospheric AOD that are based on optical extinction measurements from the Stratospheric Aerosol and Gas Experiment (SAGE) satellite instruments (Sato et al. 1993).

Monthly concentrations (ppm) of carbon dioxide are obtained for two stations: Mauna Loa, Hawaii (19°32′N, 155°35′W), and Point Barrow, Alaska (71°19′N, 156°36′W). Annual data on carbon emissions from the combustion of fossil fuels and the production of cement are from Marland et al. (Marland et al. 2001).

2.2. Statistical technique

To analyze the relationship between NDVI and the atmospheric concentration of carbon dioxide, we estimate a vector autoregression in which atmospheric CO_2 and

NDVI are endogenous and aerosol optical depth, anthropogenic carbon emissions, and time are exogenous. A structural VAR is given by

$$CO2_{mt} = \alpha_{10} + \beta_{12}NDVI_{jmt} + \phi_{11}CO2_{m-1t} + \phi_{12}NDVI_{jm-1t} + \gamma_{11}AOD_{jmt} + \gamma_{12}ECO2_t + \gamma_{13}Time + \mu_{1t}, \quad (1)$$

$$NDVI_{jmt} = \alpha_{20} + \beta_{21}CO2_{mt} + \phi_{21}CO2_{m-1t} + \phi_{22}NDVI_{jm-1t} + \gamma_{21}AOD_{jmt} + \gamma_{22}ECO2_t + \gamma_{23}Time + \mu_{2t}, \quad (2)$$

in which *CO2* is the atmospheric concentration of carbon dioxide at either Mauna Loa or Point Barrow in month *m* during year *t*; *NDVI* is the value for NDVI in grid cell *j*; *AOD* is aerosol optical depth; *ECO2* is annual anthropogenic carbon emissions; *Time* is a counter that is incremented monthly; α, β, γ, and ϕ are regression coefficients; and μ is the regression error.

Equations (1) and (2) are specified to test hypothesis number 1 and hypothesis number 2. Other variables, such as temperature, precipitation, or ENSO events, may generate the disturbances (μ) that ultimately affect both NDVI and CO_2. Indeed, the Southern Oscillation index is added to Equations (1) and (2) in section 4 to demonstrate how future research may attempt to identify variables that ultimately drive changes in NDVI and CO_2.

The notion of Granger causality focuses on disturbances to the system (μ_{1t} and μ_{2t}) and the timing in which they appear in the values of *CO2* or *NDVI*. *NDVI* is said to Granger cause *CO2* if a disturbance to *NDVI* (μ_{2t}) appears simultaneously in *CO2*. This is possible only if $\beta_{12} \neq 0$. Similarly, *CO2* is said to Granger cause *NDVI* if a disturbance to *CO2* (μ_{1t}) appears simultaneously in *NDVI*. This is possible only if $\beta_{21} \neq 0$. Based on this interpretation, statistical tests for *NDVI* Granger causes *CO2* evaluates the null hypothesis $\beta_{12} = 0$.

It is not possible to test the null hypothesis $\beta_{12} = 0$ or $\beta_{21} = 0$ directly by estimating Equations (1) and (2) because of the (possible) simultaneous relationship between *NDVI* and *CO2*. Instead, the relationship between *NDVI* and *CO2* is analyzed by estimating the VAR in standard form as follows:

$$CO2_{mt} = \psi_1 + \sum_{i=1}^{s} \xi_{1i}NDVI_{jm-it} + \sum_{i=1}^{s} \theta_{1i}CO2_{m-it} + \sum_{i=0}^{s} \sigma_{1i}AOD_{jm-it} + \lambda_1 ECO2_t + \varsigma_1 Time + \varepsilon_{1jmt}, \quad (3)$$

$$NDVI_{mt} = \psi 2 + \sum_{i=1}^{s} \xi_{2i}NDVI_{jm-it} + \sum_{i=1}^{s} \theta_{2i}CO2_{m-it} + \sum_{i=0}^{s} \sigma_{2i}AOD_{jm-it} + \lambda_2 ECO2_t + \varsigma_2 Time + \varepsilon_{2jmt}, \quad (4)$$

in which the number of possible lags is expanded relative to the first-order VAR used to illustrate the structural equations. Lag length (*s*) is determined Schwarz Bayesian criterion (Schwarz 1978), which is used to chose among lag lengths of one, two, or three. The maximum lag length of three is defined using an econometric "rule of thumb" $T^{1/3}$ in which *T* is the number of observations (22). Current

values of *AOD* are used because this variable is assumed to be exogenous (i.e., *NDVI* and/or *CO2* has no effect on *AOD*).

The relationship between atmospheric carbon dioxide and NDVI probably varies spatially and temporally over the Northern Hemisphere mid- to high-latitude growing season; therefore, Equations (3) and (4) are estimated seven times: once for each month April through October. To estimate Equation (4) for October, a maximum lag length of three includes observations of *NDVI*, *CO2*, and *AOD* for September, August, and July on the right-hand side.

To determine whether *NDVI* at grid cell *j* Granger causes *CO2* in month *m*, we estimate a restricted version of Equation (3), in which lagged values of *NDVI* are eliminated. This test is based on the assumption that $\beta_{12} = 0$ in Equation (1) or $\beta_{21} = 0$ in Equation (2) and so the null hypothesis is that there is no causal relationship. This null hypothesis is implemented statistically by restricting the ξ_{1i}'s in Equation (3) to zero as follows:

$$CO2_{mt} = \psi_1 + \sum_{i=1}^{s} \theta_{1i} CO2_{m-it} + \sum_{i=0}^{s} \sigma_{1i} AOD_{jm-it} + \lambda_1 ECO2_t + \varsigma_1 Time + \varepsilon_{1jmt}. \quad (5)$$

The lag length used to estimate Equation (5) is the same used to estimate Equation (3). To test whether *CO2* Granger causes *NDVI*, we estimate a restricted version of Equation (4) in which the lagged values of carbon dioxide are eliminated by restricting the θ_{2i}'s to zero.

Next, the null hypothesis that the regression coefficient(s) associated with the potentially causal variable in Equations (3) or (4) is zero is tested with the following statistic:

$$\omega = \frac{(RSS_r - RSS_u)/s}{RSS_u/(T-k)}, \quad (6)$$

in which *RSS* is the residual sum of squares, subscripts *r* and *u* refer to the restricted [Equation (5)] and unrestricted [Equation (3)] models of atmospheric CO_2, *T* is the number of observations, *k* is the number of regressors in Equation (3), and *s* is the number of coefficients restricted to zero in Equation (3). The test statistic ω is evaluated against an *F* distribution with *s* and $T - k$ degrees of freedom in the numerator and denominator, respectively.

Values of ω that exceed the 5% critical value reject the null hypothesis of no causal relationship. Rejecting the null hypothesis indicates the lagged values of *NDVI* have explanatory power about the current value of atmospheric carbon dioxide beyond that in the other variables in Equation (3). This information supports the alternative hypothesis; disturbances to *NDVI* at grid cell *j* Granger cause *CO2* in month *m* at either Mauna Loa or Point Barrow. Results that indicate lagged values of carbon dioxide have information about the current value of *NDVI* beyond that contained in the other variables in Equation (4) support the alternative hypothesis that disturbances to *CO2* at a monitoring station Granger cause *NDVI* at grid cell *j* in month *m*. This process is repeated for every vegetated pixel north of 30°N in North America and Eurasia and measurements of atmospheric carbon dioxide at Mauna Loa and Point Barrow during each month of the growing season.

To ensure that the results are robust, the statistical methodology is repeated with grid cells of four sizes: 1° × 1°, 2° × 2°, 3° × 3°, and 5° × 5°. Grid cells that are

1° × 1° are about 32 km on a side. This area is small relative to the terrestrial vegetation in the Northern Hemisphere, which makes it unlikely that a disturbance to the terrestrial vegetation in this area alone could generate a measurable change in the atmospheric CO_2. Instead, we assume that the disturbance generates a signal that affects other grid cells such that their combined area is able to influence measured concentrations of atmospheric carbon dioxide. At the other extreme, atmospheric concentrations at distant stations could be influenced by changes in larger grid cells, such as 5° × 5°. But such large grid cells are more likely to be occupied by a mix of land covers and experience more than one disturbance, both of which would tend to reduce the signal-to-noise ratio thereby reducing the methodology's ability to detect a causal relationship between NDVI and atmospheric CO_2. To evaluate the effect of spatial resolution on the timing and location of a causal relationship between *NDVI* and *CO2*, we compare results estimated using grid cells with four spatial resolutions.

The timing of a causal relationship applies only to the month in which the left-hand-side variable in Equation (3) or (4) is measured. For example, a causal relationship from NDVI to atmospheric carbon dioxide in June implies that atmospheric measurements of carbon dioxide in June are Granger caused by NDVI. The disturbance to NDVI that Granger causes atmospheric carbon dioxide may occur in June or in any of the previous months that are included in Equation (4). This interpretation is consistent with the relatively long periods that are required for air to move from North America or Eurasia to either Mauna Loa or Point Barrow.

2.3. Interpreting statistical significance

The statistical significance of a causal relationship, as indicated by the test statistic ω, is evaluated several ways. First, we calculate the percentage of grid cells in North America or Eurasia for which the test statistic ω exceeds the 5% threshold. Sampling theory indicates that ω should exceed the 5% threshold for about 5% of the grid cells analyzed even if there is no causal relationship between *CO2* and *NDVI*. That is, if Equation (3) is estimated with 1000 vegetated grid cells from Eurasia, sampling theory states that ω should exceed the 5% threshold for 50 grid cells. For example, 4.5% of the (2° × 2°) vegetated pixels in Eurasia (34 of the 756) show a causal relationship from *NDVI* to *CO2* at Point Barrow in April (Table 1).

To determine whether these 34 cells for which ω exceeds the 5% threshold represent a statistically meaningful causal relationship, we conduct field significance tests, which allow us to evaluate whether the causal relationships exhibited by individual pixels represent a statistically meaningful relationship at the continental scale. To do so, one needs to identify a threshold for the fraction of pixels that show a causal relationship that is greater than a fraction, which could be generated by random chance. To identify this threshold, we use Monte Carlo techniques to estimate values of ω from 1000 experimental datasets, each with 1000 grid cells. For each grid cell, we generate 22 values for *NDVI*, *CO2*, and *AOD* by drawing randomly from a normal distribution that has a mean value of zero and standard deviation of 1.0. The causal relationship between *NDVI* and CO2 for each grid cell is analyzed using the techniques described in the previous section.

Table 1. Number and percentage of grid cells in which ω rejects the null hypothesis of no causal relationship. The first values indicate the number of grid cells in which ω exceeds the 5% threshold. The second values indicate the percentage of vegetated grid cells in which ω exceeds the 5% threshold. Values in bold indicate percentages in which ω exceeds the 5% threshold simulated using Monte Carlo techniques.

		NDVI Granger causes CO_2							
		North America				Eurasia			
Site	Month	1°	2°	3°	5°	1°	2°	3°	5°
Mauna Loa	April	73/5.9%	20/6.1%	11/7.8%	6/11.3%	79/3.1%	41/5.4%	16/4.9%	2/1.6%
	May	**386/27.9%**	**73/19.0%**	**16/12.1%**	5/7.8%	**247/8.3%**	69/8.0%	24/7.7%	**15/10.1%**
	June	37/2.6%	10/2.4%	4/2.7%	3/4.0%	**458/14.3%**	**80/8.6%**	**52/13.9%**	**19/12.2%**
	July	111/7.7%	30/7.1%	9/5.9%	3/4.0%	91/2.7%	65/6.7%	19/4.9%	7/4.3%
	August	76/4.4%	19/4.4%	9/4.7%	8/7.8%	**358/8.2%**	80/7.6%	**51/11.1%**	16/7.7%
	September	118/6.6%	33/7.6%	10/5.2%	10/10.2%	**455/10.1%**	**92/8.8%**	30/6.6%	17/8.0%
	October	**226/16.0%**	**58/15.1%**	**16/11.11%**	**12/17.6%**	211/6.8%	**75/8.9%**	22/6.5%	**18/12.9%**
Point Barrow	April	77/6.2%	26/7.9%	6/4.3%	2/3.8%	163/6.3%	34/4.5%	12/3.7%	4/3.1%
	May	**111/8.0%**	30/7.8%	13/9.8%	3/4.7%	**478/16.0%**	**87/10.1%**	**31/10.0%**	13/8.8%
	June	46/3.2%	13/3.1%	4/2.7%	5/6.7%	**615/19.2%**	**138/14.8%**	31/8.3%	11/7.1%
	July	**139/9.6%**	**50/11.8%**	**16/10.4%**	8/10.8%	223/6.7%	74/7.6%	19/4.9%	13/7.9%
	August	**140/8.1%**	33/7.6%	16/8.3%	10/9.8%	**583/13.4%**	**101/9.6%**	**52/11.3%**	18/8.6%
	September	**253/14.1%**	34/7.8%	12/6.2%	5/5.1%	**431/9.6%**	**101/9.6%**	**45/9.9%**	11/5.2%
	October	**232/16.4%**	34/8.8%	13/9.0%	4/5.9%	179/5.8%	32/3.8%	**33/9.8%**	6/4.3%

Table 1. *(Continued)*

		CO_2 Granger causes NDVI							
		North America				Eurasia			
Site	Month	1°	2°	3°	5°	1°	2°	3°	5°
Mauna Loa	April	58/4.7%	13/4.0%	6/4.3%	3/5.7%	163/6.4%	55/7.2%	24/7.4%	9/7.0%
	May	79/5.7%	33/8.6%	9/6.8%	8/12.5%	168/5.6%	44/5.1%	10/3.2%	2/1.3%
	June	84/5.8%	**57/13.8%**	**17/11.4%**	**9/12.2%**	**260/8.1%**	67/7.2%	31/8.3%	10/6.4%
	July	93/6.4%	28/6.6%	17/2.0%	7/9.4%	**551/16.6%**	77/7.9%	23/5.9%	7/4.3%
	August	127/7.3%	27/6.2%	192/6.2%	**13/12.7%**	347/8.0%	59/5.6%	25/5.4%	11/5.3%
	September	142/7.9%	37/8.5%	8/4.1%	8/8.2%	271/6.0%	67/6.4%	37/8.1%	21/9.9%
	October	84/5.9%	26/6.7%	5/3.5%	2/2.9%	183/5.9%	49/5.8%	14/4.1%	8/5.7%
Point Barrow	April	98/7.9%	20/6.1%	7/5.0%	**7/13.2%**	203/7.9%	56/7.4%	325/8.0%	8/6.2%
	May	**226/16.3%**	**50/13.0%**	33/25.0%	**9/14.1%**	**391/13.1%**	42/4.9%	310/3.9%	9/6.1%
	June	**241/16.7%**	**53/12.8%**	**22/14.8%**	8/10.8%	176/5.5%	54/5.8%	18/4.8%	10/6.4%
	July	**138/9.5%**	26/6.1%	6/3.9%	6/8.1%	229/6.9%	45/4.6%	22/5.7%	10/6.1%
	August	**268/15.4%**	21/4.8%	**21/10.9%**	8/7.8%	**350/8.0%**	58/5.5%	20/4.3%	11/5.3%
	September	**197/11.0%**	36/8.3%	19/9.8%	8/8.2%	262/5.8%	74/7.1%	24/5.3%	14/6.6%
	October	**142/10.1%**	28/7.3%	**16/11.1%**	2/2.9%	169/5.5%	56/6.6%	21/6.2%	10/7.2%

For each experimental dataset, we record the number of grid cells for which ω exceeds the 5% critical value. Values for the 1000 datasets are ranked in descending order. The value in position 50, 82, represents a 5% significance level—only 5% of the time do 8.2% (or more) of the grid cells have a value for ω greater than the 5% critical value when no causal relationship is present in the data-generating process. This percentage is used as a threshold in a field significance test that identifies months when and regions (North America or Eurasia) where there is a causal relationship between *NDVI* and *CO2* for the entire field when the field consists of about 1000 grid cells. Because we repeat the analysis with grid cells of different sizes, we repeat the Monte Carlo simulations with 400, 150, and 75 grid cells in each of the 1000 datasets. The 5% thresholds are 9.2% (400 grid cells), 10% (150 grid cells), and 12% (75 grid cells).

The degree to which conclusions about a causal relationship between *CO2* and *NDVI* are robust is assessed by comparing results across the four spatial scales: $1° \times 1°$, $2° \times 2°$, $3° \times 3°$, and $5° \times 5°$. Only if the percentage of grid cells for which ω exceeds the 5% critical value is greater than the threshold simulated by Monte Carlo techniques for two or more of the four spatial scales do we conclude that there is a statistically meaningful causal relationship between *CO2* and *NDVI* for a given month, region (North America or Eurasia), and monitoring station (Mauna Loa or Point Barrow).

The statistical significance of the causal relationship also is evaluated by the spatial distribution of the grid cells. If only about 5% of the grid cells have a value for ω that exceeds the 5% critical value, we would expect these grid cells to be scattered randomly in space. Conversely, if the percentage of grid cells that has a value for ω that exceeds the field significance test, this relationship may be concentrated in space. Consistent with these expectations, the 4.5% of the $2° \times 2°$ grid cells that have a causal effect on the atmospheric concentration of carbon dioxide at Point Barrow in April are scattered across Eurasia (Figure 1), while the 19% of North American grid cells that have a causal effect on the atmospheric concentration of carbon dioxide at Mauna Loa in May are grouped tightly (Figure 2).

To determine whether the geographic distribution of grid cells that have a causal relationship is random, their distribution among land covers is compared to the area of land covers. If the geographic distribution of grid cells that show a causal relationship is random, we would expect these grid cells to be distributed among land covers roughly in proportion to the geographic area of these land covers. For example, 21.2% of the $2° \times 2°$ Eurasian grid cells that have a causal effect on the atmospheric concentration of carbon dioxide at Point Barrow in April are classified as evergreen needleleaf forest, which constitutes 21.9% of the vegetated grid cells in Eurasia. This result reinforces the notion that the 4.5% the $2° \times 2°$ Eurasian grid cells for which ω exceeds the 5% critical value does not represent a statistically meaningful causal relationship.

Conversely, if the percentage of grid cells that shows a causal relationship between *NDVI* and *CO2* in a given land cover greatly exceeds the percentage of vegetated grid cells classified as this land cover, such spatial concentration could reinforce the conclusion about a causal relationship that is based on the percentage of vegetated grid cells for which ω exceeds the 5% critical value. Returning to the 19% of North American grid cells for which the value of ω exceeds the 5% critical value at Mauna Loa in May, 26.7% of these grid cells are classified as mixed

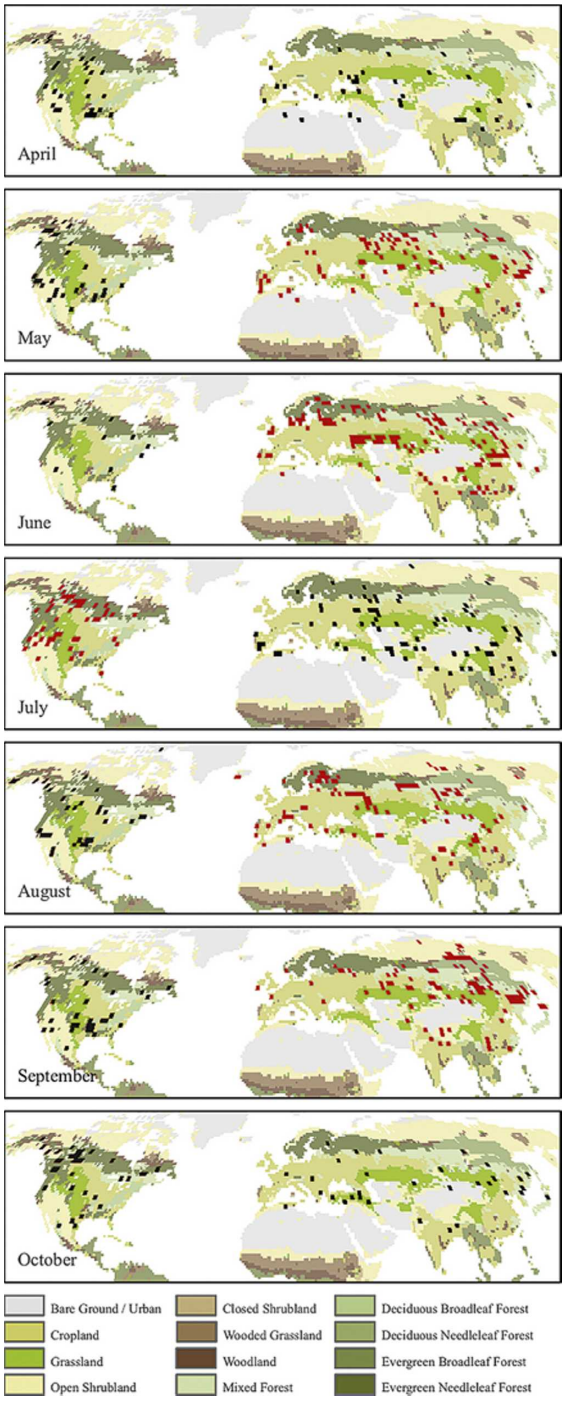

Figure 1. The location of 2° × 2° grid cells where the value of ω rejects the null hypothesis that NDVI Granger causes atmospheric concentrations of carbon dioxide as measured at Point Barrow, Alaska. Months in which the percentage of grid cells in North America or Eurasia that rejects this null hypothesis exceeds the 5% threshold simulated by the Monte Carlo techniques are given in red.

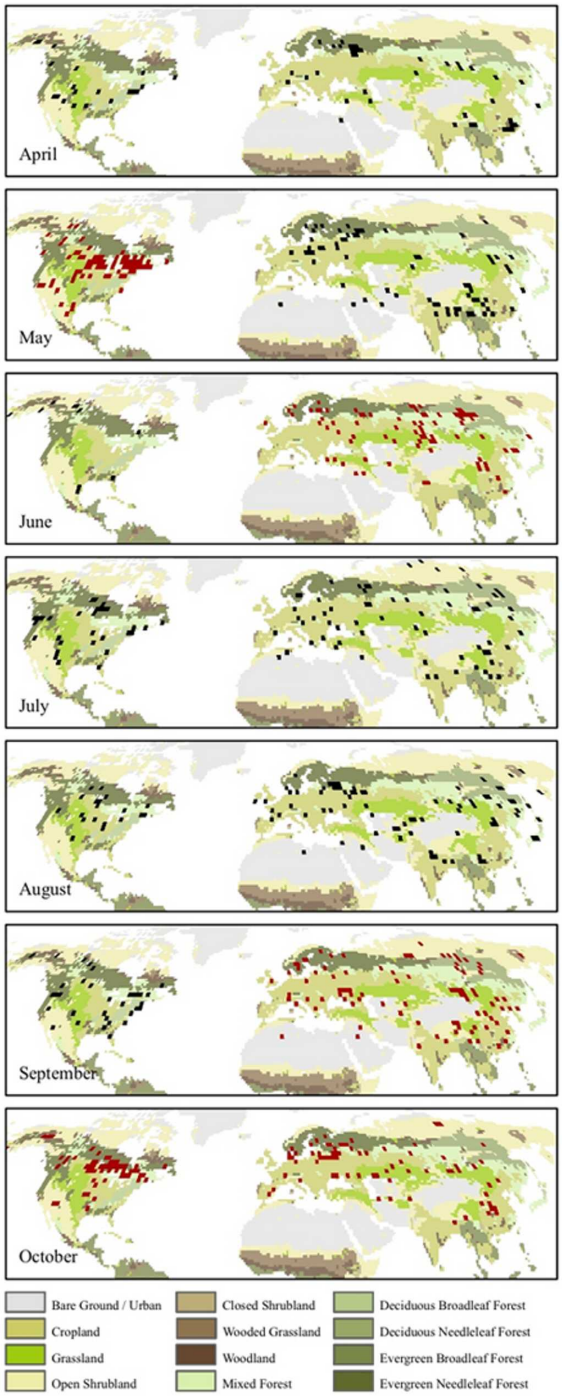

Figure 2. The location of 2° × 2° grid cells where the value of ω rejects the null hypothesis that NDVI Granger causes atmospheric concentrations of carbon dioxide as measured at Mauna Loa, Hawaii. Months in which the percentage of grid cells in North America or Eurasia that rejects this null hypothesis exceeds the 5% threshold simulated by the Monte Carlo techniques are given in red.

forests, which account for 11.9% of vegetated grid cells in North America. This spatial concentration reinforces the notion that North American *NDVI* Granger causes *CO2* measured at Mauna Loa during May. Again, Monte Carlo techniques are used to simulate a threshold for field significance tests that determines whether the geographic distribution of grid cells that shows a causal relationship is consistent with a random process.

3. Results

3.1. NDVI Granger causes carbon dioxide

Based on the percentage of vegetated grid cells that show a causal relationship, results from two or more spatial scales indicate that Eurasian *NDVI* Granger causes *CO2* measured at Point Barrow during May, June, August, and September (Table 1 and Figure 1). Similarly, Eurasian values of *NDVI* Granger cause *CO2* measured at Mauna Loa in May, June, August, September, and October (Figure 2). In North America, *NDVI* Granger causes *CO2* measured at Point Barrow during July only. At Mauna Loa, there is a causal relationship from North American *NDVI* to CO_2 during May and October.

Some of these causal relationships appear to be concentrated in land covers (Table 2). In North America, a disproportionate percentage of the grid cells that have a causal effect on *CO2* measurements at Mauna Loa in May are classified as mixed forests or croplands (Figure 2). In October, a disproportionate percentage of the grid cells in North America that have a causal effect on atmospheric concentrations of carbon dioxide at Mauna Loa are classified as mixed forests or evergreen needleleaf forests. Similarly, evergreen needleleaf forests account for a disproportionate percentage of North American grid cells that show a causal effect on atmospheric measurements of carbon dioxide at Point Barrow during July (Figure 1).

Similar concentrations appear in Eurasia. A disproportionate percentage of the Eurasian grid cells where NDVI Granger causes atmospheric carbon dioxide at Point Barrow are located in evergreen needleleaf forests (June and August) and deciduous needleleaf forests (September). The causal effect of Eurasian NDVI on atmospheric concentrations of carbon dioxide at Mauna Loa in August is concentrated in croplands.

3.2. Carbon dioxide causes NDVI

Based on the percentage of vegetated grid cells that show a causal relationship at two or more spatial scales, *CO2* Granger causes *NDVI* in North America only (Table 1). At Point Barrow, *CO2* Granger causes *NDVI* in North America during May, June, August, and October (Figure 3). At Mauna Loa, there is a causal relationship from *CO2* to North American *NDVI* during June only (Figure 4). For Eurasia, *CO2* Granger causes *NDVI* at a single scale for some months, but there are no months during which this causal relationship is present at two or more spatial scales.

When present, the causal effect of atmospheric carbon dioxide on North American NDVI generally is distributed among land covers in rough proportion to their

Table 2. Geographic distribution of grid cells where NDVI Granger causes CO_2. The first value in the parentheses indicates the percentage of grid cells in a particular land cover. The second number indicates the 5% critical value that identifies the percentage of grid cells that show a causal relationship that would be found in the land cover if these grid cells were distributed randomly among land covers. ENF = evergreen needleleaf forest, EBF = evergreen broadleaf forest, DNF = deciduous needleleaf forest, DBF = deciduous broadleaf forest, MF = mixed forest, WD = woodland, WDG = wooded grassland, CSB = closed shrub land, OSB = open shrub land, GRS = grassland, CRP = cropland.

		North America											
Site	Month	ENF (21.9%/ 31.7%)	EBF (0.0%/ 0.0%)	DNF (0.0%/ 0.0%)	DBF (4.6%/ 8.3%)	MF (11.4%/ 18.3%)	WD (1.9%/ 5.0%)	WDG (0.1%/ 1.7%)	CSB (0.15%/ 1.7%)	OSB (17.6%/ 25.0%)	GRS (13.2%/ 20.0%)	CRP (18.8%/ 26.7%)	Other (10.4%/ 18.3%)
Mauna Loa	April	8.8%			7.5%	6.3%	3.8%	25.0%	20.0%	8.8%	20.0%		
	May*	6.2%			9.9%	26.7%	0.3%	9.6%	7.5%	27.7%	12.0%		
	June	22.5%				12.5%	10.0%			10.0%	5.0%		40.0%
	July	40.8%			3.3%	0.8%				5.8%	16.7%	17.5%	15.0%
	August	23.7%			3.9%	17.1%					13.2%	34.2%	7.9%
	September	21.2%			6.1%	10.6%	3.8%			8.3%	9.1%	20.5%	20.5%
	October*	33.2%			2.6%	22.8%	2.2%			7.3%	1.7%	22.0%	8.2%
Point Barrow	April	21.2%				5.8%	5.8%			27.9%	1.0%	30.8%	7.7%
	May	15.8%			0.8%	3.3%	6.7%			39.2%	8.3%	16.7%	9.2%
	June	28.8%				17.3%	7.7%			19.2%		3.8%	23.1%
	July*	35.0%			0.5%	15.0%	0.5%		0.5%	16.5%	11.5%	14.5%	6.0%
	August	11.4%			3.8%	16.7%	2.3%		0.8%	28.8%	9.1%	11.4%	15.9%
	September	22.1%			10.3%	9.6%	0.7%			19.9%	14.0%	12.5%	11.0%
	October	28.7%			5.1%	20.6%				14.0%	8.8%	14.0%	8.8%

Table 2. *(Continued)*

		Eurasia											
Site	Month	ENF (6.9%/ 12.2%)	EBF (0.8%/ 2.2%)	DNF (4.3%/ 8.9%)	DBF (0.4%/ 1.1%)	MF (13.7%/ 20.0%)	WD (0.8%/ 3.3%)	WDG (0.3%/ 1.1%)	CSB (0.1%/ 1.1%)	OSB (11.0%/ 17.8%)	GRS (15.7%/ 21.1%)	CRP (33.2%/ 40.0%)	Other (12.8%/ 17.8%)
Mauna Loa	April	17.7%	4.9%	2.4%	0.6%	19.5%	0.6%			4.3%	10.4%	35.4%	4.3%
	May	10.9%	2.9%	1.4%		7.6%	1.1%		0.4%	3.6%	14.1%	45.3%	12.7%
	June*	10.9%		5.9%	0.6%	14.1%	2.2%			13.4%	15.0%	26.9%	10.9%
	July	10.4%	0.4%	8.1%	0.4%	10.4%	1.2%		1.2%	11.9%	11.5%	33.5%	11.2%
	August	3.4%		4.7%	0.3%	10.0%	0.3%		0.6%	10.9%	10.6%	42.8%	16.3%
	September*	7.3%	1.1%	9.2%	0.3%	6.0%	1.9%	0.5%	0.5%	12.0%	15.8%	32.3%	13.1%
	October*	9.3%	0.3%	2.0%	0.3%	10.0%				11.0%	16.3%	39.3%	11.3%
Point Barrow	April	1.5%	1.5%		2.9%	4.4%	0.7%			14.0%	15.4%	28.7%	30.9%
	May*	4.0%		6.3%		17.5%	0.3%			6.3%	15.2%	35.9%	14.4%
	June*	11.1%	1.4%	2.7%		15.8%	0.2%	0.4%	0.5%	9.1%	19.9%	29.7%	9.2%
	July	4.1%		0.7%	1.0%	9.1%	1.0%	1.0%	0.3%	16.9%	14.9%	31.8%	19.3%
	August*	12.4%		1.5%	0.2%	16.6%	0.2%	0.5%		14.4%	11.6%	27.5%	15.1%
	September*	2.2%		16.6%	0.5%	18.6%	1.5%			11.9%	16.6%	23.3%	8.9%
	October	3.9%		1.6%	1.6%	15.6%	0.8%			5.5%	27.3%	25.8%	18.0%

* Months in which the percentage of grid cells for which the value of ω exceeds the 5% critical value simulated by Monte Carlo techniques.

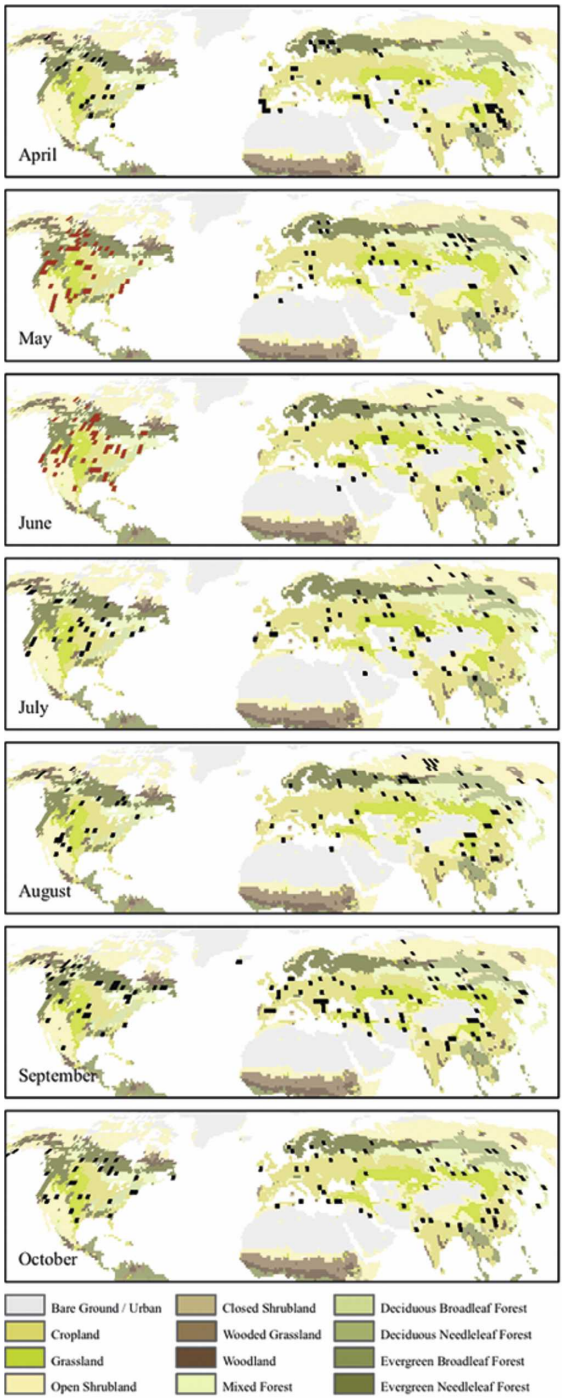

Figure 3. The location of 2° × 2° grid cells where the value of ω rejects the null hypothesis that atmospheric concentrations of carbon dioxide at Point Barrow, Alaska, Granger cause NDVI. Months in which the percentage of grid cells in North America or Eurasia that rejects this null hypothesis exceeds the 5% threshold simulated by the Monte Carlo techniques are given in red.

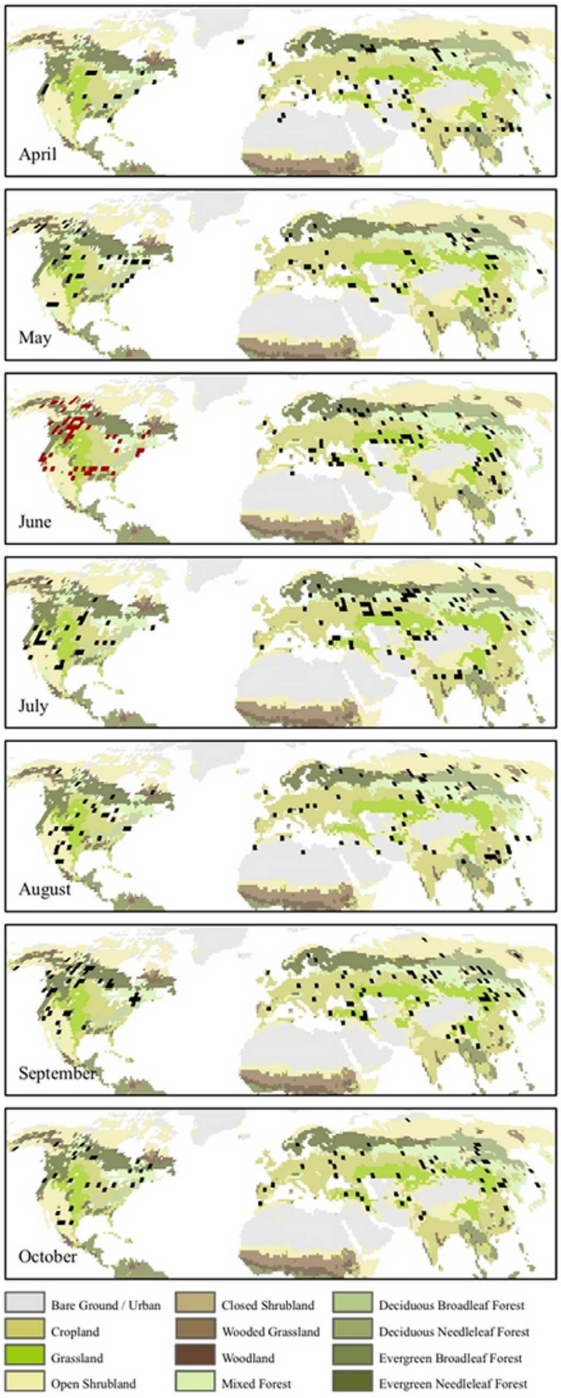

Figure 4. The location of 2° × 2° grid cells where the value of ω rejects the null hypothesis that atmospheric concentrations of carbon dioxide at Mauna Loa, Hawaii, Granger cause NDVI. Months in which the percentage of grid cells in North America or Eurasia that rejects this null hypothesis exceeds the 5% threshold simulated by the Monte Carlo techniques are given in red.

geographic extent. The sole exception is the causal effect of *CO2* measured at Point Barrow on June values of North American *NDVI*, which is concentrated in cropland (Table 2).

4. Discussion

To facilitate the discussion, we clarify the interpretation of Granger causality relative to previous results. For this analysis, Granger causality identifies locations where disturbances to *NDVI* generate changes in the atmospheric *CO2* in a particular month or locations where disturbances to the atmospheric concentration of carbon dioxide generate changes in NDVI during a particular month. A causal effect of *NDVI* on *CO2* is not equivalent to efforts to identify locations that contribute to the intra-annual cycle of atmospheric carbon dioxide (e.g., Randerson et al. 1997; Gurney et al. 2002). For example, Randerson et al. (Randerson et al. 1997) argue that seasonal variations in the atmospheric concentration of carbon dioxide at stations north of 55°N, including Point Barrow, are associated with tundra, boreal forests, and other northern ecosystems. If these areas are relatively undisturbed, no causal relationship will be indicated because lagged values of *CO2* in Equation (3) will embody the intra-annual pattern.

4.1. NDVI Granger causes atmospheric carbon dioxide

Red squares in Figures 1 and 2 indicate that it is possible to map the relationship between disturbances to terrestrial vegetation, as measured by NDVI, and measurements of CO_2 at distant monitoring stations, such as Mauna Loa and Point Barrow. This result rejects hypothesis number 1 that Northern Hemisphere observational sites are not sensitive to changes in the CO_2 seasonal flux cycle except at close proximity (Murayama et al. 2004). This implies that historical records at observational sites can be used to understand the effect of the terrestrial biota on atmospheric CO_2.

The timing and location of the causal relationship from NDVI to atmospheric carbon dioxide at Mauna Loa can be compared to those reported by Buermann et al. (Buermann et al. 2007). In contrast to their results, which indicate little correlation between Eurasian *NDVI* and amplitude of the growing season cycle, there is a causal relationship for June, September, and October. These months correspond to the start and end of the Northern Hemisphere warm season, which is roughly consistent with the time that masses from Eurasia dominate Mauna Loa (Lintner et al. 2006). North American air masses have their greatest presence at Mauna Loa during July/August; nonetheless, a causal relationship between *NDVI* and *CO2* appears outside this window, May and October.

Conclusions regarding the land covers that affect atmospheric CO_2 also differ. Buermann et al. (Buermann et al. 2007) find a correlation between the amplitude of the seasonal cycle at Mauna Loa and North American grass- and cropland NDVI. A causal relationship from *NDVI* to *CO2* is present in North American croplands during May, but does not extend to grasslands, which make up 13.2% of vegetated pixels but account for only 7.5% of the pixels that show a causal relationship in May (Table 2). The causal relationship in October is spread among

land covers in a way that is cannot be differentiated from a random distribution. Similarly, the causal relationship in Eurasia is spread evenly among land covers.

These differences can be understood several ways. As described previously, correlation is a much weaker indicator than Granger causality. This weakness is exacerbated by the critical values used to establish correlation. Buermann et al. (Buermann et al. 2007) use critical values from one-tailed tests to evaluate their results. The null hypothesis of a one-tailed test is that the coefficient is zero against an alternative that it is either positive or it is negative (one or the other). This null hypothesis is inconsistent with their tests, For example, Figure 2 in Buermann et al. (Buermann et al. 2007) shows both positive and negative correlations, and the one-tailed test is applied to both sides of zero in Figures 3 and 4. Given these comparisons, critical values should be taken from a two-tailed test, which evaluates the null hypothesis that the correlation coefficient is zero against an alternative that it can be either positive or negative (both outcomes are possible). Using a one-tailed test generates significance level half their true value—the 10% level described in Figure 2 is really only the 20% level. This implies that there is a one in five chance of observing the results shown in Figure 2e (in Buermann et al. 2007) even if there is no correlation between NDVI and the growing season amplitude at Mauna Loa.

Furthermore, the repeated nature of their regressions implies that 20% of their pixels (using the reported 20% significance level) should show a correlation with the amplitude of NDVI. Visual inspection of Figure 2e from Buermann et al. (Buermann et al. 2007) indicates that about 20% of the pixels analyzed show a correlation between NDVI and atmospheric carbon dioxide. Under these conditions, correlations reported by Buermann et al. (Buermann et al. 2007) may not pass a field significance tests and therefore probably do not support a statistically meaningful relationship between NDVI and the growing season amplitude at Mauna Loa.

4.2. Atmospheric carbon dioxide Granger causes NDVI

Enhanced levels of carbon dioxide can increase photosynthesis by increasing the carboxylation rate of the enzyme Rubisco and by inhibiting the oxygenation of Ribulose-1,5biphosphate (Drake et al. 1997). These positive effects may be enhanced in areas where water limits plant growth because elevated levels of atmospheric carbon dioxide also increase water use efficiency. Figures 3 and 4 indicate that atmospheric concentrations of carbon dioxide at Mauna Loa and Point Barrow Granger cause NDVI in North America during May and/or June. These results are the first statistically meaningful large-scale empirical confirmation of a CO_2 fertilization effect.

We say first statistically meaningful large-scale empirical confirmation because much of the existing evidence comes from experiments in growth chambers or simple statistical analyses. A meta-analysis of chamber experiments indicates that elevated levels of carbon dioxide increase total biomass and net CO_2 assimilation (Curtis and Wang 1998). These results generally are confirmed by a meta-analysis of free-air CO_2 enrichment experiments, which indicates that elevated levels of carbon dioxide increase light-saturated carbon uptake, and diurnal carbon uptake, and that these effects are greatest in trees and are smallest in C_3 grasses (Ainsworth and Long 2005).

Efforts to confirm these effects using large-scale observations are difficult because factors other than carbon dioxide may limit plant growth and/or the methods used may not be able to disentangle the timing of multiple changes in the linked atmosphere–vegetation system. For example, the CO_2 fertilization effect may be difficult to detect on a large scale if it is muted in some areas by the availability of nitrogen (Oren et al. 2001). Similarly, current and lagged correlations among atmospheric carbon dioxide, NDVI, temperature, and precipitation described by Lim et al. (Lim et al. 2004) are difficult to interpret because their specification does not differentiate between correlation and causation and is estimated from a relatively small sample, 1982–92.

Our results do not support arguments that the CO_2 fertilization effect will be concentrated in space based on physiological mechanisms that promote it. Here, grid cells that show a causal relation are distributed among land covers in rough proportion to the spatial extent of land covers. This is not consistent with arguments that the effects of elevated levels of atmospheric CO_2 should be positively (Polglase and Wang 1992) or negatively (Alexandrov et al. 2003) related to temperature.

4.3. Illustrating unmodelled effects: The role of El Niño events

The statistical models represented by Equations (1) and (2) are designed to test the two hypotheses regarding the relationship between atmospheric *CO2* and *NDVI*. Based on this purpose, the statistical models are simple and omit variables that may constitute the disturbances to *NDVI* (μ_{1t}) and *CO2* (μ_{2t}), which create the causal relationships between the terrestrial biota and atmospheric carbon dioxide.

We demonstrate the effect of omitted variables by adding the Southern Oscillation index (Allen et al. 1991) to Equations (1) and (2) and repeating the analysis. We focus on ENSO events because they are exogenous to the coupled atmosphere–terrestrial biosphere system and disturb both terrestrial vegetation (Buermann et al. 2003) and atmospheric carbon dioxide (Bacastow 1976; Francey et al. 1995; Keeling et al. 1995; Kaufmann et al. 2006).

If ENSO events generate disturbances that are responsible for a causal relationship between *CO2* and *NDVI*, including the Southern Oscillation index will weaken the finding of causality because the source of the disturbances, ENSO events, remains in the restricted form of the equation. That is, if ENSO events disturb *NDVI*, which then affect *CO2*, eliminating *NDVI* from Equation (3) will not increase its residual sum of squares because the predictive power of *NDVI* remains in Equation (5) as embodied in the Southern Oscillation index. Consistent with this expectation, including the Southern Oscillation index reduces the months when and locations where there is a causal relationship between *NDVI* and *CO2*. There is only one month in which *NDVI* Granger causes *CO2* at two or more spatial scales. Eurasian *NDVI* Granger causes September measurements of atmospheric *CO2* at Point Barrow in September. There is no month in which *CO2* Granger causes NDVI at more than one resolution. Together, these results suggest that ENSO events disturb *NDVI* and the atmospheric concentration of carbon dioxide and these disturbances are responsible for the causal relationship with the other variable.

5. Conclusions

The simple models described here allow us to reject the null hypothesis that there is no link between the terrestrial biota and CO_2 measured at distant monitoring stations and vice versa. This indicates that is it possible to link changes in the terrestrial biota, as measured by NDVI, to atmospheric concentrations of carbon dioxide at distant monitoring stations. Furthermore, there is some preliminary evidence for the effect of elevated carbon dioxide on terrestrial vegetation. We say preliminary because we cannot be sure whether the innovations in atmospheric CO_2 affect plants directly or share the same climate signal with NDVI.

To investigate the factors that disturb atmospheric CO_2 and NDVI, future efforts will use a methodology suggested by the effect of omitted variables. By adding variables to Equations (1) and (2), we will test hypotheses about the factors that affect the atmospheric concentration of carbon dioxide at Mauna Loa and other monitoring stations. For example, including climate variables in Equation (1) may allow us to identify months when and locations where changes in surface temperature or precipitation affect vegetation in a way that changes the intra-annual cycle of atmospheric CO_2. Furthermore, by recovering the coefficients in the primitive VAR [Equations (1) and (2)], we may be able to differentiate between the net effects of changing climate on photosynthesis and heterotrophic respiration.

References

Ainsworth, E. A., and S. P. Long, 2005: What have we learned from 15 years of free–air CO_2 enrichment (FACE)? A meta-analytic review of the responses of photosynthesis, canopy properties, and plant production to rising CO_2. *New Phytol.,* **165,** 351–372.

Alexandrov, G. A., T. Oikawa, and Y. Yamagata, 2003: Climate dependence of the CO2 fertilization effect on terrestrial net primary production. *Tellus,* **55B,** 669–675.

Allen, R. J., N. Nicholls, P. D. Jones, and I. J. Butterworth, 1991: A further extension of the Tahiti-Darwin SOI, early ENSO events and Darwin pressure. *J. Climate,* **4,** 743–749.

Bacastow, R. B., 1976: Modulation of atmospheric carbon dioxide by the Southern Oscillation. *Nature,* **261,** 116–118.

Buermann, W., B. Anderson, C. J. Tucker, R. E. Dickinson, W. Lucht, C. S. Potter, and R. B. Myneni, 2003: Interannual covariability in Northern Hemisphere air temperatures and greenness associated with El Niño–Southern Oscillation and the Arctic Oscillation. *J. Geophys. Res.,* **108,** 4396, doi:10.1029/2002JD002630.

——, B. R. Lintner, C. D. Koven, A. Angert, J. E. Pinzon, C. J. Tucker, and I. Y. Fung, 2007: The changing carbon cycle at Mauna Loa observatory. *Proc. Natl. Acad. Sci. USA,* **104,** 4249–4254.

Chapin, F. S., S. A. Zimov, G. R. Shaver, and S. E. Hobbie, 1996: CO_2 fluctuations at high latitudes. *Nature,* **383,** 585–586.

Curtis, P. S., and X. Wang, 1998: A meta-analysis of elevated CO_2 effects on woody plant mass, form, and physiology. *Oecologia,* **113,** 299–313.

Drake, B. G., M. A. Gonzalez, S. P. Meier, and S. P. Long, 1997: More efficient plants: A consequence of rising atmospheric CO_2? *Annu. Rev. Plant Physiol. Plant Mol. Biol.,* **48,** 609–639.

Francey, R. J., P. P. Tans, C. E. Allison, I. G. Enting, J. W. C. White, and M. Trolier, 1995: Changes in oceanic and terrestrial carbon uptake since 1982. *Nature,* **373,** 326–330.

Granger, C. W. J., 1969: Investigating causal relations by econometric models and cross-spectral methods. *Econometrica,* **37,** 424–438.

Gurney, K. R., and Coauthors, 2002: Towards robust regional estimates of CO_2 sources and sinks using atmospheric transport models. *Nature,* **415,** 626–630.

Gutman, G., 1999: On the use of long-term global data of land reflectances and vegetation indices derived from the Advanced Very High Resolution Radiometer. *J. Geophys. Res.,* **104,** 6241–6255.

Holben, B. B., 1986: Characteristics of maximum-value composite images from temporal AVHRR data. *Int. J. Remote Sens.,* **7,** 1417–1434.

Kaufmann, R. K., L. Zhou, R. B. Myneni, C. J. Tucker, D. Slayback, N. V. Shabanov, and J. Pinzon, 2003: The effect of vegetation on surface temperature: A statistical analysis of NDVI and climate data. *Geophys. Res. Lett.,* **30,** 2137, doi:10.1029/2003GL018251.

——, R. D. D'Arrigo, C. Laskowski, R. B. Myneni, L. Zhou, and N. K. Davi, 2004: The effect of growing season and summer greenness on northern forests. *Geophys. Res. Lett.,* **31,** L09205, doi:10.1029/2004GL019608.

——, H. Kauppi, and J. H. Stock, 2006: Emissions, concentrations, and temperature: A time series analysis. *Climatic Change,* **77,** 249–278.

Keeling, C. D., T. P. Whorf, M. Wahlen, and J. Vanderplicht, 1995: Interannual extremes in the rate of rise of atmospheric carbon dioxide since 1980. *Nature,* **375,** 666–670.

——, J. F. S. Chin, and T. P. Whorf, 1996: Increased activity of northern vegetation inferred from atmospheric CO2 observations. *Nature,* **382,** 146–149.

Kohlmaier, G. F., E. O. Sire, and A. Janecek, 1989: Modeling the seasonal contribution of a CO_2 fertilization effect of the terrestrial vegetation to the amplitude increase in atmospheric CO_2 at Mauna Loa observatory. *Tellus,* **41B,** 487–510.

Lim, C., M. Kafatis, and P. Megonigal, 2004: Correlation between atmospheric CO_2 concentration and vegetation greenness in North America: CO_2 fertilization effect. *Climate Res.,* **28,** 11–22.

Lintner, B., W. Buerman, C. Koven, and I. Y. Fung, 2006: Seasonal circulation and Mauna Loa CO_2 variability. *J. Geophys. Res.,* **111,** D13104, doi:10.1029/2005JD006535.

Marland, G., T. A. Boden, and R. J. Andres, cited 2001: Global, regional, and national fossil fuel CO_2 emissions. Trends online: A compendium of data on global climate change, Carbon Dioxide Information Analysis Center, Oak Ridge National Laboratory, Oak Ridge, TN. [Available online at http://cdiac.ornl.gov/trends/emis/meth_reg.htm.]

Morimoto, S., T. Nakazawa, K. Higuchi, and S. Aoki, 2000: Latitudinal distribution of atmospheric CO_2 sources and sinks inferred by $\delta^{13}C$ measurements from 1985 to 1991. *J. Geophys. Res.,* **105,** 24 315–24 326.

Murayama, S., S. Taguchi, and K. Higuchi, 2004: Interannual variation in the atmospheric CO_2 growth rate: Role of atmospheric transport in the Northern Hemisphere. *J. Geophys. Res.,* **109,** D02305, doi:10.1029/2003JD003729.

Myneni, R. B., F. G. Hall, P. J. Sellers, and A. L. Marshak, 1995: The meaning of spectral vegetation indices. *IEEE Trans. Geosci. Remote Sens.,* **33,** 481–486.

——, C. D. Keeling, C. J. Tucker, G. Asrar, and R. R. Nemani, 1997a: Increased plant growth in the northern high latitudes from 1981 to 1991. *Nature,* **386,** 698–702.

——, R. R. Nemani, and S. W. Running, 1997b: Algorithm for the estimation of global land cover, LAI and FPAR based on radiative transfer models. *IEEE Trans. Geosci. Remote Sens.,* **35,** 1380–1393.

——, and Coauthors, 2001: A large carbon sink in the woody biomass of Northern Forests. *Proc. Natl. Acad. Sci. USA,* **98,** 14 784–14 789.

Nemani, R. R., C. D. Keeling, H. Hashimoto, W. M. Jolly, S. C. Piper, C. J. Tucker, R. B. Myneni, and S. W. Running, 2003: Climate driven increases in terrestrial net primary production from 1982 to 1999. *Science,* **300,** 1560–1563.

Oren, R., and Coauthors, 2001: Soil fertility limits carbon sequestration by forest ecosystems in a CO_2-enriched atmosphere. *Nature,* **411,** 469–471.

Polglase, P. J., and Y. P. Wang, 1992: Potential CO_2-enhanced carbon storage by the terrestrial biosphere. *Aust. J. Bot.,* **40,** 641–656.

Randerson, J. T., M. V. Thompson, T. J. Conway, I. Y. Fung, and C. B. Field, 1997: The contribution of terrestrial sources and sinks to trends in the seasonal cycle of atmospheric carbon dioxide. *Global Biogeochem. Cycles,* **11,** 535–560.

Sato, M., J. E. Hansen, M. P. McCormick, and J. B. Pollack, 1993: Stratospheric aerosol optical depths, 1850–1990. *J. Geophys. Res.,* **98,** 22 987–22 994.

Schwarz, G., 1978: Estimating the dimension of a model. *Ann. Stat.,* **6,** 461–464.

Wang, W., B. T. Anderson, N. Phillips, R. K. Kaufmann, C. Potter, and R. B. Myneni, 2006: Feedbacks of vegetation on summertime climate variability over the North American grasslands. Part I: Statistical analysis. *Earth Interactions,* **10.** [Available online at http://EarthInteractions.org.]

Zhou, L., C. J. Tucker, R. K. Kaufmann, D. Slayback, N. V. Shabanov, and R. B. Myneni, 2001: Variations in northern vegetation activity inferred from satellite data of vegetation index during 1981 to 1999. *J. Geophys. Res.,* **106,** 20 069–20 083.